

Positive-Unlabeled Learning for Control Group Construction in Observational Causal Inference

1 Ilias Tsoumas
2

3 Artificial Intelligence Group,
4 Wageningen University and Research
5 The Netherlands
6 BEYOND Centre, National
7 Observatory of Athens
8 Greece
9 i.tsoumas@noa.gr

10 Athanasios Askopoulos
11 BEYOND Centre, National
12 Observatory of Athens
13 Greece

14 Dimitrios Bompoudakis
15 BEYOND Centre, National
16 Observatory of Athens
17 Greece

18 Andreas Kalogeris
19 BEYOND Centre, National
20 Observatory of Athens
21 Greece

22 Vasileios Sitokonstantinou
23 Image Processing Laboratory (IPL),
24 University of Valencia
25 Spain

26 Ioannis Athanasiadis
27 Artificial Intelligence Group,
28 Wageningen University and Research
29 The Netherlands

30 Charalampos (Haris) Kontoes
31 BEYOND Centre, National
32 Observatory of Athens
33 Greece

34 true value. This work has important implications for observational
35 causal inference, especially in fields where randomized experiments
36 are difficult or costly. In domains such as earth, environmental, and
37 agricultural sciences, it enables a plethora of quasi-experiments by
38 leveraging available earth observation and climate data, particularly
39 when treated units are available but control units are lacking.

Keywords

Causality, Machine Learning, Propensity Score, Treatment

ACM Reference Format:

Ilias Tsoumas, Dimitrios Bompoudakis, Vasileios Sitokonstantinou, Athanasios Askopoulos, Andreas Kalogeris, Ioannis Athanasiadis, and Charalampos (Haris) Kontoes. 2025. Positive-Unlabeled Learning for Control Group Construction in Observational Causal Inference. In *Proceedings of 3rd Workshop on Causal Inference and Machine Learning in Practice (KDD 2025 Workshop)*. ACM, New York, NY, USA, 17 pages. <https://doi.org/XXXXXXX.XXXXXXX>

1 Introduction

In modern science, when a randomized controlled trial is not a feasible option, we turn to observational studies to answer causal questions. The most common type of these questions is of the form "*What is the effect of intervention T on outcome Y?*". The average treatment effect (ATE) is a popular quantity that we estimate to answer these types of questions. Inferring causal ATE estimates of an intervention on any outcome formally requires access to control and treated units. Equally important for observational causal inference is the capability to adjust for other variables that are involved as confounders in the intervention-outcome system of interest, so that any difference in outcome between control and treated groups to be attributed only to the intervention.

The absence of treated or control group data is a critical concern. Molinari [10] presents how we can realize estimation of ATE if

Abstract

In causal inference, whether through randomized controlled trials or observational studies, access to both treated and control units is essential for estimating the effect of a treatment on an outcome of interest. When treatment assignment is random, the average treatment effect (ATE) can be estimated directly by comparing outcomes between groups. In non-randomized settings, various techniques are employed to adjust for confounding and approximate the counterfactual scenario to recover an unbiased ATE. A common challenge, especially in observational studies, is the absence of units clearly labeled as controls—that is, units known not to have received the treatment. To address this, we propose positive-unlabeled (PU) learning as a framework for identifying, with high confidence, control units from a pool of unlabeled ones, using only the available treated (positive) units. We evaluate this approach using both simulated and real-world data. We construct a causal graph with diverse relationships and use it to generate synthetic data under various scenarios, assessing how reliably the method recovers control groups that allow estimates of true ATE. We also apply our approach to real-world data on optimal sowing and fertilizer treatments in sustainable agriculture. Our findings show that PU learning can successfully identify control (negative) units from unlabeled data based only on treated units and, through the resulting control group, estimate an ATE that closely approximates the

Permission to make digital or hard copies of all or part of this work for personal or classroom use is granted without fee provided that copies are not made or distributed for profit or commercial advantage and that copies bear this notice and the full citation on the first page. Copyrights for components of this work owned by others than the author(s) must be honored. Abstracting with credit is permitted. To copy otherwise, or republish, to post on servers or to redistribute to lists, requires prior specific permission and/or a fee. Request permissions from permissions@acm.org.

KDD 2025 Workshop, Toronto, CA

© 2025 Copyright held by the owner/author(s). Publication rights licensed to ACM.
ACM ISBN 978-x-xxxx-xxxx-x/YYY/MM
<https://doi.org/XXXXXXX.XXXXXXX>

we do not know what the treatment status of a part of the units. Kuzmanovic et al. propose how to estimate conditional average treatment effects (CATE) [7] with missing treatment information. Beyond effect estimation under settings with partial absence of treatment information, Lancaster & Imbens [8], building on [17], show that even when some control units are mistakenly classified and may have actually received the treatment—what they refer to as "contaminated controls"—it is still possible to recover unbiased estimates, as long as this misclassification is properly modeled in the analysis. Additionally, Rosenbaum & Rubin exploit the availability of a pool of potential controls on building a balanced control group using multivariate matching methods that incorporate the propensity score, ensuring similarity between treated and control units based on observed covariates [13].

In this work, we focus on the case of the absolute absence of units that are clearly labeled as controls—that is, units known not to have received the treatment. To address this issue, we propose the use of positive-unlabeled (PU) learning [1] as a formal framework for causal effect estimation in the absence of control units. Specifically, we identify, with high confidence, control units from a pool of unlabeled ones, using only the available treated (positive) units. Quite recently, PU learning has been proposed as a methodological solution to identify reliable control units from a pool of unlabeled one [20]. In, parallel Kato et al. [5] propose a novel end-to-end PU learning method to estimate ATE in settings with a lack of control units. Complementary, with this work we especially contribute to this conceptual proposition through the following: i. Use PU learning to construct a reliable control group from unlabeled data delinked from the effect estimation step. In this way, we facilitate the use of any causal model and adjustment set in the effect estimation part instead of the end-to-end solution of [5]. ii. We compare the use of an adjustment set defined by the back-door criterion for training the PU learner with a more exhaustive feature set that also includes *bad controls*—such as mediators, colliders, and even the outcome variable itself, and show that the latter yields superior performance. iii. We perform experiments with simulated and real-world data around sustainable agriculture to showcase the usefulness of our approach. These contributions aim to showcase the PU learning as a useful addition to the observational causal inference toolbox, specifically when real-world interventions have taken place, but we lack of labeled control units to realise an experiment. Especially, it applies in the domains of earth, environmental and agricultural sciences, where given the availability of earth observation and meteoclimatic data it can unlock a plethora of quasi-experiments, as we showcase in our real-world examples.

2 Preliminaries & Problem Formulation

2.1 Observational Causal Inference

For each of the experimental setups that follow, simulated or real-world, we employ the relevant causal directed acyclic graph $G = (V, A)$ which includes all involved variables as vertices V connected through directed edges E and represent the causal relationships within the relevant treatment T - outcome Y system, e.g., the fertilizer - yield system. We limited all setups to binary treatments $T \in \{1, 0\}$ and we aim to estimate their unbiased effects on an outcome of interest Y . We choose the exact adjustment set $Z \subseteq V$,

if any, that satisfies the back-door criterion relative to (T, Y) , blocking every path from T to Y that contains an arrow into T , and no descendant nodes from Z to T are allowed. Then, we retrieve *ATE* as shown in Eq. 1 based only on observational quantities.

$$\begin{aligned} \text{ATE} &= \mathbb{E}[Y | do(T = 1)] - \mathbb{E}[Y | do(T = 0)] \\ &= \sum_z (\mathbb{E}[Y | T = 1, Z = z] - \mathbb{E}[Y | T = 0, Z = z]) \cdot P(Z = z) \end{aligned} \quad (1)$$

The capability to retrieve the *ATE*, whether we express it in Equation 1 through as a structural causal model [11], or we express it via potential outcomes framework [14], rests on some fundamental assumptions that both frameworks directly or indirectly rely on:

$$\text{Unconfoundedness: } Y(t) \perp\!\!\!\perp T \mid Z \quad \forall t \in \{0, 1\} \quad (2)$$

$$\text{Positivity: } 0 < P(T = t \mid Z = z) < 1 \quad \forall t \in \{0, 1\}, \forall z \in Z \quad (3)$$

$$\text{Consistency: } Y = Y(t) \quad \text{if } T = t \quad (4)$$

Firstly, it is the stable unit treatment value assumption (SUTVA) that requires there are (i) no interference between units, i.e., one unit's outcome is unaffected by other units' treatment, and (ii) well-defined treatment with no different forms of each treatment level. The unconfoundedness assumption (Eq. 2) requires all confounders are measured, and conditioning on them to removes bias. The positivity assumption (Eq. 3) requires every unit has a positive probability of receiving each treatment level given adjustment set Z . The consistency assumption (Eq. 4) requires that when we observe $T = t$, the observed outcome Y is equal to the outcome that would result from an intervention setting T to t through $do(\cdot)$ operator.

2.2 PU learning for control group construction

In this causal inference context, we should properly define the notation and slightly reformulate the assumptions of PU learning for the case of control group identification. In general, the typical target of PU learning is to learn a binary classifier using only a set of labeled positive instances and a set of unlabeled instances which include both positive and negative instances. In this work, we instrumentalize the PU learning framework as the means to recover from unlabeled units using only positive-treated units a subset of reliable negative-control units, for the downstream task of effect estimation.

Thus, the target variable is the true class label, which in our case is the treatment $T \in \{1, 0\}$ that indicates the real state of unit, where $T = 1$ indicates a real treated/positive and $T = 0$ indicates a real control/negative. X represents the feature vector that describes all units and will be used to estimate T . A critical innovation we propose and explore in this work is that X does not need to be limited to the aforementioned adjustment set Z ; instead, in our formulation X may contain any covariate included in V (from causal graph G that will be beneficial for a robust estimator of T) and even variables exogenous of G system that will be useful. So we state that $Z \subseteq V \subseteq X$. The variable that differentiates the notation from typical supervised learning is a third variable $S \in \{1, 0\}$, which differs from T that represents the real state of unit in terms of whether it has received or not treatment, S is a label indicator. The $S = 1$ indicates that the unit is observed/annotated

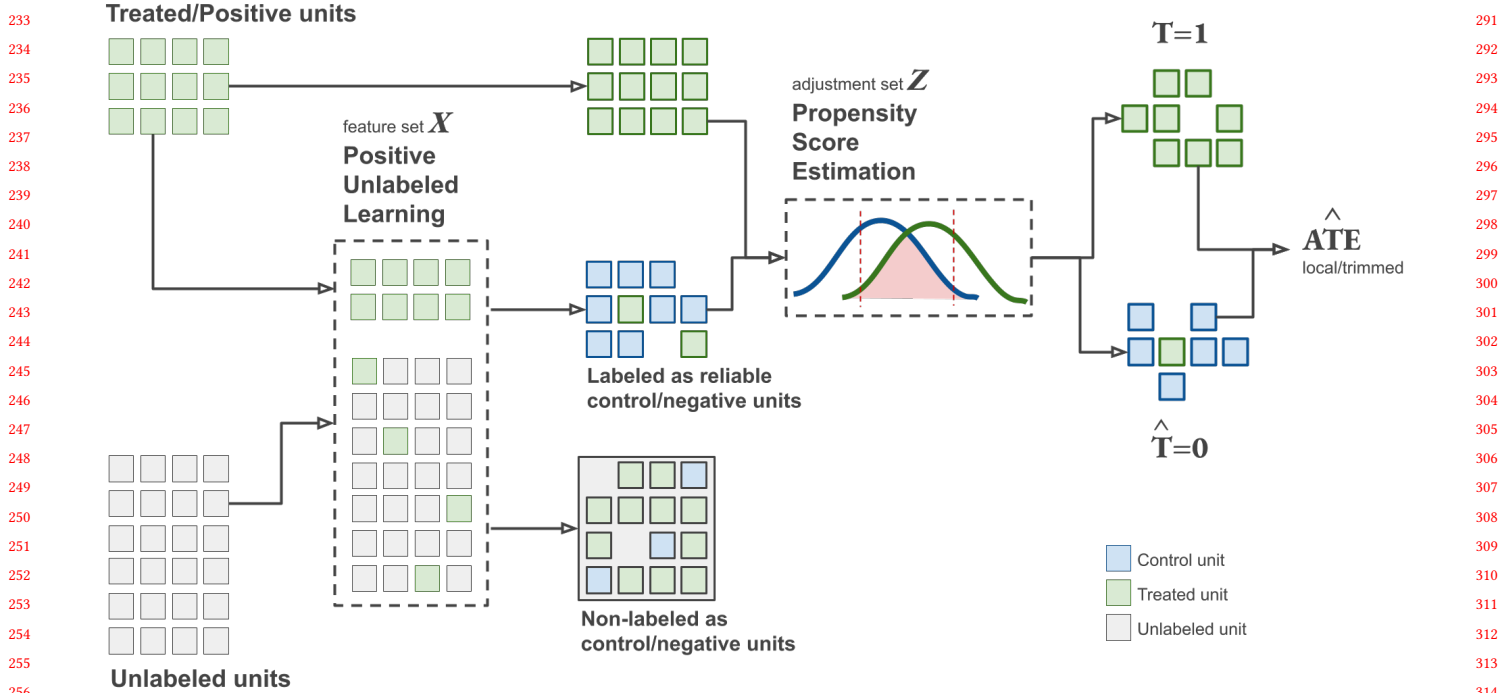


Figure 1: Overview of the use of PU learning as a preparatory step for causal estimation tasks that lack control groups.

as treated/positive and $S = 0$ indicates that unit is unlabeled, so it can be either a control/negative or a treated/positive.

$$\text{SCAR: } P(S = 1 | T = 1, X) = P(S = 1 | T = 1) = c \quad c \in (0, 1) \quad (5)$$

$$\text{No Label Noise in Treated: } P(T = 0 | S = 1) = 0 \quad (6)$$

$$\text{Controls in Unlabeled Set: } P(T = 0 | S = 0) > 0 \quad (7)$$

Separability:

$$P(t = 1 | x) = \sigma(f(x)) \gg 0.5 \quad \text{for most } x \in \text{Treated}$$

$$P(t = 0 | x) = \sigma(f(x)) \ll 0.5 \quad \text{for most } x \in \text{Controls} \quad (8)$$

Smoothness:

$$\|x - x'\| < \epsilon, \text{ for small } \epsilon > 0 \quad (9)$$

$$\Rightarrow P(y = 1 | x) \approx P(y = 1 | x')$$

The selected completely at random (SCAR) assumption (Eq. 5) states that labeled positives are selected uniformly at random from all treated units, and selection for labeling is independent of features. The Eq. 6 implies that there is no possibility of mislabeling, e.g. a unit labeled as treated to be truly control. The Eq. 7 requires at least a control unit to be included in the unlabeled dataset. The separability assumption (Eq. 8) state that there exists a decision function $f(x)$ that reliably separates the two classes among unlabeled units via score thresholding (ie $\sigma(\cdot)$ denotes the sigmoid function). The smoothness assumption (Eq. 9) that two units with nearby feature vectors x x' shared the same treatment status, which forces us to allow post-treatment and exogenous features to be included in X . Finally, the proposed end target of PU learner is to estimate the treatment assignment probability $P(T = 1 | X)$ which allows to

derive units that strongly looks truly untreated given its features (Eq. 10) that can be used as controls in causal effect estimation.

$$P(T = 0 | X) = 1 - P(T = 1 | X) \gg 0.5 \quad (10)$$

3 Methodology & Experimentation

In this section, we describe in more detail: i. how we employ PU learning as a preparatory step to construct a reliable control group in the case of its absence to enable causal effect estimation and ii. the four experimental setups - two simulated and two real-world datasets - where we test our idea.

3.1 Framework for control group construction

As Fig. 1 illustrates, we emphasize cases where treated and unlabeled units are available, in single-training-set scenarios either with simulated or real-world datasets, because we focus mainly in earth, environmental and agriculture cases where dominantly the units are pieces of land (e.g. agricultural parcels) that belong on the same population/dataset and either they receive an intervention/event or we do not know if they receive it or not. Specifically, we use a 2-step technique. In the first step we leverage the SPY method [9] where some of the real treated units are turned into spies, which we "hide" in the unlabeled dataset. A Naive Bayes classifier is trained, considering the unlabeled units as controls. Then, we label as "reliable" control units those for which the posterior probability is lower than the lowest of spies. In the second step, we employ iterative SVM (iSVM) [21]. In each iteration, an SVM classifier is trained using the real treated units and the reliable controls from the first step. The unlabeled units that are classified as controls by this classifier are

then added to the set of reliable controls for the next iteration till no class change occurs between two iterations. Thus, we categorize the unlabeled units into two groups: the reliable control units, in which the PU learning assigned the control label with a tunable confidence; and the group with units that were left unlabeled because they do not differ enough from the real treated given features X . We do not consider the latter as treated because we already have a group with confirmed real treated units, so there is no reason to risk to add bias with some possible false labeled units as treated. Naturally, these two new groups will probably contain some false labeled units.

Afterwards, we train a propensity score estimator (i.e. a logistic regression) with the real treated units and the labeled from PU learning as reliable controls. However, we have already chosen the adjustment set Z that satisfies the backdoor criterion based on the relevant causal graph G that represents the system relationships for the estimation of the effect of T on Y and we train the propensity score estimator only using this subset of X , the adjustment set Z . We plot the propensity scores per group and we trim the scores of the two groups to ensure sufficient overlap between them. This trimming ensures that we avoid an extrapolation in regions with little comparability between groups, and we focus on *ATE* estimation on the region of common support. Given that we have recovered as reliable controls the units that, intuitively speaking, significantly differ from the real treated for the PU learning estimator, which is trained on X and in parallel we estimate propensity scores training an estimator on Z , it is clear that we risk drastic shrinkage of units in the area of overlap between the two groups due to the significant overlap of feature sets $Z \subseteq X$. This area of overlap is prone to be the area of the smallest propensity scores, given that reliable controls are units that are based on X place in a conceptually similar area from the PU learning estimator. Consequently, an issue arises about how strong the positivity assumption holds each time and what exactly this strong '*trimmed*' or '*local*' *ATE* quantity represents. Finally, we estimate the *ATE* with several estimators using the trimmed, based on propensity scores, treated and reliable control groups for reasons of completeness and framework assessment. We use linear regression and distance matching as baseline estimation methods, and Inverse Propensity Score Weighting (IPW) [18] and the causal machine learning method T-learner [6].

3.2 Experimental setups & data

We simulate data under two different assumptions (generating $n = 1000$ samples for each), one with linear and one with non-linear causal relationships, to test our ideas in a fully controllable environment. For this purpose, we construct the causal graph G_{sim} of Fig. 2 where we employ the Cinelli et al. work [2] in order to introduce G_{sim} a wide palette of different relationships '*confounders*', '*mediators*', '*colliders*'. Specifically, vertices $V_{good} = \{X_{1.1}, X_{1.2}, X_{2.1}, X_{2.2}, U_3\}$ are '*good controls*' reducing bias by blocking back-door paths if we control for them. The $V_{bad} = \{X_3, X_5, X_7, X_9, M\}$ are '*bad controls*', with addition of X_3 as control would lead to '*bias amplification*'. The X_5 are known as '*M-bias*' that induce bias through U_1, U_2 . M mediates the effect we want to estimate, so we keep this path untouched without controlling for this variable, similarly to X_7 , where a control for it is equivalent to a partial

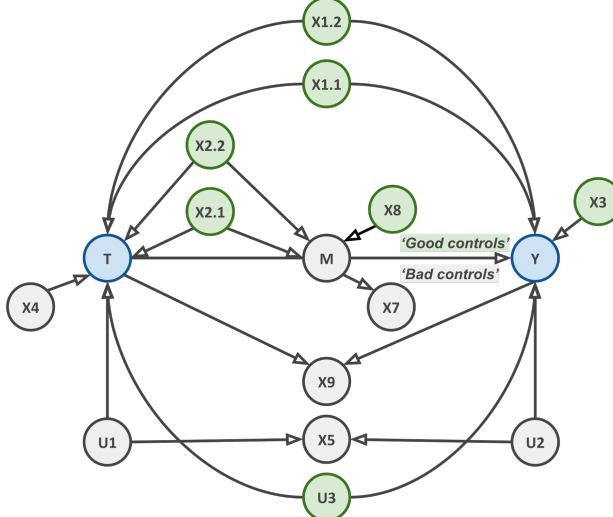


Figure 2: The causal graph G_{sim} serves as the data-generating process for both linear and non-linear simulations.

control for mediator M . X_9 is a typical '*bad control*' because controlling for it opens a colliding path and induces '*selection bias*'. Finally, vertices $V_{neutral} = \{X_3, X_8\}$ are neutral in terms of inserting or removing bias but can be useful controls in terms of *ATE* precision. Thus, as expected from graph construction, the minimum adjustment set Z_{sim} that satisfies the back-door criterion contains the '*good controls*' so $Z_{sim} = V_{good} = \{X_{1.1}, X_{1.2}, X_{2.1}, X_{2.2}, U_3\}$ for an unbiased estimation of *ATE* of treatment T on outcome Y of causal system G_{sim} . The Sec. B of the Appendix present the data-generating process in detail.

Also, we investigate the applicability of our ideas in two real-world scenarios from the domain of sustainable agriculture. First, we use the causal graph, data and causal effect estimation setup from Tsoumas et al. work [19]. They estimate the *ATE* of treatment T : whether the cotton field is sown on an annotated date as favorable or not, on the outcome Y , which is the final yield of cotton. We use the adjustment set $Z_{sowing} = \{\text{Weather on sowing date, Soil moisture on sowing date, Topsoil properties, Topsoil organic carbon, Seed variety, Geometry of field}\}$ that satisfies the back-door criterion of their proposed causal graph, and also we use the additional available variables $V_{extra} = \{\text{Crop growth, Location \& area of field, Harvest date \& cultivation period, Yield}\}$ that are not used for effect estimation in order to test the use of an expanded feature set $X_{sowing} = Z_{sowing} + V_{extra}$ over the adjustment set Z_{sowing} to construct a group of reliable control units and the hold of the positivity assumption. As a second real-world scenario, we introduce a new dataset about the impact of a digestate fertilizer (i.e., a sustainable alternative to chemical fertilizers) on wheat biomass in fields cultivated with durum wheat. For this paper, we adopt the popular example of fertilization-yield causal graph from Pearl's book [12], incorporate it with the richer ground truth causal graph in [16] regarding soil processes. In this dataset, the adjustment set and the feature set are composed as follows: $Z_{fertilizer} = \{\text{Topsoil organic carbon, Accumulated precipitation, Growing degree days, Accumulated vegetation moisture content, Soil moisture, Soil type Seed}\}$

465	466	Dataset	PU method	Feature Set	# Positives (true treated)	# Spies	# Unlabeled				Evaluation Metrics				523				
							controls		treated		# Selected		# Non-selected		Control Recall	Control Precision	Contamination Rate	Treated Leakage	
							# Controls	# Treated	# Controls	# Treated	Recall	Precision	Rate	Leakage					
467	468	Linear	SPY	Z	346	103 (30%)	505	149	334	31	171	118	0.661	0.915	0.085	0.208	524		
				X					505	28	0	121	1.000	0.947	0.053	0.188	525		
			SPY+iSVM	Z	365	109 (30%)	478	157	143	4	362	145	0.283	0.973	0.027	0.027	526		
				X					505	0	0	149	1.000	1.000	0	0	527		
469	470	Non-linear	SPY	Z	365	109 (30%)	478	157	186	28	292	129	0.389	0.870	0.131	0.178	528		
				X					476	15	2	142	0.996	0.969	0.031	0.095	529		
			SPY+iSVM	Z	35	5 (15%)	121	15	121	16	357	141	0.253	0.883	0.117	0.102	530		
				X					474	0	4	157	0.992	1.000	0	0	531		
471	472	Sowing	SPY	Z	35	5 (15%)	121	15	92	3	29	12	0.760	0.968	0.032	0.200	532		
				X					72	4	49	11	0.595	0.947	0.053	0.267	533		
			SPY+iSVM	Z	23	3 (15%)	99	11	97	5	24	10	0.802	0.951	0.049	0.333	534		
				X					101	5	20	10	0.835	0.953	0.047	0.333	535		
473	474	Fertilization	SPY	Z	23	3 (15%)	99	11	64	3	35	8	0.646	0.955	0.045	0.273	536		
				X					71	5	28	6	0.717	0.934	0.066	0.455	537		
			SPY+iSVM	Z	87	8	12	3	89	7	10	4	0.899	0.927	0.073	0.636	538		
				X					87	8	12	3	0.878	0.916	0.084	0.727	539		

Table 1: Summary of control group selection using SPY and SPY+iSVM across four datasets (Linear, Non-linear, Sowing, Fertilization), evaluated with feature sets Z (adjustment set) and X (the most informative variables set about treatment).

variety} and $X_{sowing} = Z_{sowing} + \{Exogenous\ organic\ matter\ indexes, Produced\ biomass\ proxy\}$. More details about the effect estimation and the data in the Table 3 on Sec. A of Appendix.

4 Results

In this section we present & discuss the results of our experiments regarding the proposed utilization of PU learning as an enabler of any causal effect estimation task when a confirmed control group is completely absent, but a source of unlabeled units is available.

For the evaluation of the framework, we emulate PU conditions through the popular '*hide and seek*' approach [15]. Specifically, we engineer positive-unlabeled datasets from the aforementioned simulated and real-world positive-negative datasets. We do this simply by hiding a percentage of positive/treated units within the negative/control units, something that allows us to consider this mixed group with units from both treatment classes as an unlabeled set to test our ideas. This satisfies the SCAR assumption (Eq. 5) and facilitates the assessment of the PU learner using common binary classification evaluation metrics. However, we have to clarify some slight conceptual changes from typical classification metrics that better align with and reflect a causal inference context. While throughout the paper we refer to treated units as positives and controls as negatives in the PU learning setup, during evaluation, we treat true controls as the positive class to assess how well the method recovers clean / reliable control units. Thus, for clarity, under this evaluation perspective, True Positives (TP) correspond to true control units correctly recovered as controls, False Positives (FP) correspond to treated units wrongly selected as controls, False Negatives (FN) to true control units that were not recovered and True Negatives (TN) to treated units correctly not selected (held out as no control units). Thus, we use: the Control Recall equation (Eq. 11) to assess how many of the true controls were recovered (it measures the coverage of the control group); the Control Precision equation (Eq. 12), which summarizes how many were actual controls out of selected as 'reliable controls'; the Contamination Rate (Eq. 13), which refers to the proportion of selected as 'reliable controls' that were actually treated; and we introduce the Treated Leakage metrics (Eq. 14) that measures how many units mistakenly ended up in 'reliable controls' among true treated units.

$$\text{Control Recall} = \frac{TP}{TP + FN} \quad (11)$$

$$\text{Control Precision} = \frac{TP}{TP + FP} \quad (12)$$

$$\text{Contamination Rate} = \frac{FP}{TP + FP} \quad (13)$$

$$\text{Treated Leakage} = \frac{FP}{FP + TN} \quad (14)$$

In Table 1, the evaluation metrics of PU learning for retrieving real control units from an unlabeled pool of mixed control and treated units are presented in detail for the four different datasets. In the two simulated, linear and non-linear, datasets our results show that the combination of SPY with iSVM returns the best results in all metrics with the use of X feature set instead of Z adjustment set. The use of X extremely outperforms in any metric, with more significant gains in the almost elimination of any leakage of treated in the 'reliable controls' and the increase of recall. Even SPY method alone using X outperforms the combined solution of SPY and iSVM when they are trained on Z. In the sowing and fertilization datasets, recall and precision follow almost the same fluctuations as in the simulated data. However, leakage of treated units presents a slight increase with the use of the feature set X in comparison with the adjustment set Z. Furthermore, the fertilization dataset, when SPY and iSVM are trained on X presents very high treated leakage, with 8 out of 11 hidden treated units classified as controls, which risks significantly biasing the results of the following effect estimation task. A likely explanation is the very small sample size of spies and hidden treated units for the machine learning task.

In all datasets, the number of retrieved 'reliable controls' tend to be more if the larger X feature set is used for PU learning - column '# Selected' in Table 1. After the trimming of both groups' units based on propensity scores to secure treated and control units have overlapped propensities, it appears (in the column '(treated, control)' of Table 2) that bigger overlap between groups emerges in the more complex 2-steps setup (SPY plus iSVM with the use of X feature set). This is also visualized in Sec. C of the Appendix , where the propensity scores overlap for all datasets are depicted. Due to the skewed propensity scores distribution of inferred reliable controls even for the best case (i.s. SPY plus iSVM with X) of

581	582	Dataset	Control Units	(treated, control)	true effect	PU Feature Set	Causal Effect Estimation Methods											
							Linear Regression			IPW weighting			Matching			T-Learner(RF)		
							ATE	CI	p-value	ATE	CI	p-value	ATE	CI	p-value	ATE	CI	p-value
583	584	Linear	real controls	(495, 505) - no trim	-	Z	3.664 (3.447, 3.895)	0.000	3.848 (3.451, 4.237)	0.001	3.927 (3.601, 4.192)	0.001	4.029 (3.939, 4.119)	0.001	4.029 (3.939, 4.119)	-	639	
			SPY	(36, 232)	3.000	X	2.718 (2.250, 3.143)	0.000	3.081 (1.927, 4.121)	0.001	3.261 (2.648, 3.620)	0.001	3.520 (3.211, 3.828)	0.001	3.520 (3.211, 3.828)	-	640	
			SPY+iSVM	(450, 414)		Z	2.800 (2.631, 2.997)	0.000	2.818 (2.337, 3.376)	0.001	3.282 (2.989, 3.392)	0.001	3.520 (3.428, 3.630)	0.001	3.520 (3.428, 3.630)	-	641	
			(22, 147)	(414, 424)		X	2.757 (2.109, 3.338)	0.000	3.231 (1.817, 4.500)	0.001	3.667 (2.906, 4.250)	0.001	3.771 (3.331, 4.212)	0.001	3.771 (3.331, 4.212)	-	642	
585	586	Non-linear	real controls	(522, 478) - no trim	-	Z	3.021 (2.861, 3.185)	0.000	3.188 (2.765, 3.559)	0.001	3.574 (3.320, 3.726)	0.001	3.814 (3.720, 3.909)	0.001	3.814 (3.720, 3.909)	-	643	
			SPY	(17, 77)	9.525	X	8.057 (5.989, 10.452)	0.000	7.775 (4.819, 10.827)	0.001	7.209 (4.660, 8.793)	0.001	7.261 (6.322, 8.201)	0.001	7.261 (6.322, 8.201)	-	644	
			(513, 487)	(86, 137)		Z	9.480 (9.100, 9.886)	0.000	9.570 (9.040, 10.035)	0.001	9.321 (8.900, 9.607)	0.001	9.324 (9.132, 9.516)	0.001	9.324 (9.132, 9.516)	-	645	
			SPY+iSVM	(513, 470)		X	7.962 (6.762, 8.993)	0.000	7.884 (6.269, 9.466)	0.001	7.556 (6.318, 8.178)	0.001	7.877 (7.384, 8.371)	0.001	7.877 (7.384, 8.371)	-	646	
587	588	Sowing	real controls	(50, 121)	-	Z	9.717 (9.367, 10.094)	0.000	9.799 (9.296, 10.229)	0.001	9.597 (9.155, 9.869)	0.001	9.829 (9.646, 10.011)	0.001	9.829 (9.646, 10.011)	-	647	
			SPY	(13, 92)	expected	X	2.11 (-479, 902)	0.544	315 (-487, 1024)	0.138	244 (-733, 1099)	0.226	259 (-134, 653)	0.001	259 (-134, 653)	-	648	
			(14, 14)	(25, 43)	positive	Z	664 (-267, 1596)	0.147	811 (122, 1660)	0.030	689 (-54, 1369)	0.063	777 (376, 1178)	0.001	777 (376, 1178)	-	649	
			SPY+iSVM	(39, 47)		X	156 (-463, 776)	0.615	322 (-25, 724)	0.087	293 (-145, 723)	0.128	300 (82, 530)	0.001	300 (82, 530)	-	650	
589	590	Fertilization	real controls	(34, 99) - no trim	-	Z	546 (211, 880)	0.002	471 (138, 816)	0.001	448 (186, 760)	0.006	372 (215, 528)	0.024	372 (215, 528)	0.024	651	
			(8, 38)	(20, 47)	expected	X	211 (-600, 6599)	0.097	315 (-173, 4351)	0.094	244 (-1188, 2842)	0.219	259 (-903, 1947)	0.001	259 (-903, 1947)	-	652	
			(24, 67)	(31, 67)	positive	Z	2.342 (-0.168, 4.851)	0.067	0.805 (-711, 2.604)	0.167	0.425 (-1.173, 2.268)	0.345	0.464 (-0.363, 1.292)	0.001	0.464 (-0.363, 1.292)	-	653	
			SPY+iSVM	(31, 67)		X	1.302 (-0.566, 3.170)	0.168	1.190 (-0.391, 2.843)	0.076	0.981 (-0.426, 3.142)	0.162	0.542 (-0.228, 1.312)	0.001	0.542 (-0.228, 1.312)	-	654	
591	592		real controls	(34, 99) - no trim	-	Z	1.188 (-0.386, 2.762)	0.138	1.160 (-0.094, 2.649)	0.055	0.708 (-0.834, 2.266)	0.200	1.104 (0.484, 1.725)	0.001	1.104 (0.484, 1.725)	-	655	
			(8, 38)	(24, 67)	expected	X	3.000 (-0.600, 6.599)	0.097	1.866 (-0.173, 4.351)	0.094	1.111 (-1.188, 2.842)	0.219	0.903 (-0.141, 1.947)	0.001	0.903 (-0.141, 1.947)	-	656	
			SPY+iSVM	(31, 67)		Z	2.342 (-0.168, 4.851)	0.067	0.805 (-711, 2.604)	0.167	0.425 (-1.173, 2.268)	0.345	0.464 (-0.363, 1.292)	0.001	0.464 (-0.363, 1.292)	-	657	
			(31, 67)	(31, 67)		X	1.750 (0.003, 3.498)	0.049	1.322 (-0.347, 3.122)	0.047	0.742 (-0.555, 2.265)	0.192	0.823 (0.158, 1.488)	0.001	0.823 (0.158, 1.488)	-	658	

Table 2: Effect estimation using treated units and (i) real control, (ii) retrieved reliable controls under various PU learning methods, feature sets, and ATE estimation techniques.

sowing and fertilization datasets, we apply asymmetric trimming to retain units with estimated propensity scores in the range [0.1, 0.6]. This decision ensures that we operate within a region of the covariate space where there is reasonable overlap between positively labeled treated units and inferred control candidates. However, this approach limits our estimand to an *ATE* within this low- to moderate-propensity subpopulation. Consequently, our *ATE* estimates are not directly generalizable to the full population or to high-propensity treated units, which are trimmed out due to lack of comparable control analogs. While this trimming reduces the risks of extrapolation and positivity violation, it introduces a form of selection bias and may underestimate the true heterogeneity of treatment effects across the broader covariate space. So, in terms of proper classification/reliable controls identification, the full 2-step PU learning method outperforms the use of SPY alone in most cases and the superiority of use of *X* feature set instead of *Z* adjustment set for the PU learning is profound. In the Sec. D of the Appendix we included a slope chart per dataset that compares the top-15 features in terms of influence and their change between the iSVM trained on *Z* and *X*, using model coefficients as feature importance.

However, as a final evaluation step given in reality we have control units for each dataset, we leverage various methods from different methodological backgrounds to estimate the causal *ATE* of each treatment on the outcome of interest before and after the retrieval of control units through our proposed solution. Observing the results in Table 2, we easily summarize for the two simulated and the sowing datasets that the setup with SPY and iSVM model trained on the feature set *X* succeeds in retrieving a statistically significant *ATE* very close to that is retrieved by the confirmed treated & control groups with all different causal estimators. Also, we observe that in the cases where *Z* is used in PU learning, we have an underestimate of *ATE* and lacking of statistical significance, probably due to extremely large trimming [0.1, 0.3] that isolate our estimation to a limited subpopulation and also leads to a very small number of units left in both groups.

For the fertilization dataset, the results are less stable (Table 2). Using the real control units, we observe a positive *ATE*, though not statistically significant. After applying the PU learning method –

specifically the more robust SPY plus iSVM plus *X* scenario – we observe a slight increase in *ATE* estimates, with linear regression and IPW yielding statistically significant results (*p*-value < 0.05), and matching and T-Learner producing similar outcomes. However, these results should be interpreted with caution due to high treated leakage in this scenario. Additionally, we applied our method to a real unlabeled dataset, enriched with available confirmed controls, to identify reliable units and estimate the *ATE* using only these controls (ignoring their actual treatment status) and the treated group. This dataset includes 616 unlabeled units and 99 confirmed controls. Using the SPY plus iSVM plus *X* method and trimming the propensity scores to the range [0.05, 0.6] to ensure overlap, we identified 67 reliable controls, 55 of which are confirmed controls. Once again, the results align with those obtained using only real controls or engineered pseudo-unlabeled data (Table 2). Specifically, for the real unlabeled dataset: linear regression estimated an *ATE* of 1.641 (*CI* : [-0.393, 3.675], *p* = 0.112); IPW estimated an *ATE* of 1.255 (*CI* : [-0.613, 3.002], *p* = 0.113); matching yielded an *ATE* of 1.207 (*CI* : [-0.709, 2.528], *p* = 0.133); and the T-Learner produced an *ATE* of 0.877 (*CI* : [0.075, 1.679]). Overall, even in this less reliable setting of the fertilization dataset, the results suggest that our PU learning approach can effectively recover the true *ATE* in the absence of a known control group.

5 Conclusions

In this work, we proposed, implemented, and evaluated the use of PU learning as a reliable approach for identifying control units from unlabeled data, addressing the challenge of missing confirmed controls. Our experiments demonstrate that, under appropriate configurations—such as avoiding restrictions on effect estimation covariates when training the PU learner—this approach can be effective. Further work should examine the trimming–extrapolation trade-off, explore using $P(T = 1|X)$ to enrich the treated group, apply more advanced PU methods, and test on causal effect benchmarks. Ultimately, we provide a simple, practical, and realistic solution that can unlock a wide range of quasi-experiments in earth, environmental, and agricultural sciences, especially given the growing availability of large-scale earth observation data.

References

- [1] Jessa Bekker and Jesse Davis. 2020. Learning from positive and unlabeled data: A survey. *Machine Learning* 109, 4 (2020), 719–760.
- [2] Carlos Cinelli, Andrew Forney, and Judea Pearl. 2024. A crash course in good and bad controls. *Sociological Methods & Research* 53, 3 (2024), 1071–1104.
- [3] Maxence Dodin, Florent Levavasseur, Antoine Savoie, Lucie Martin, Jean Foulon, and Emmanuelle Vaudour. 2023. Sentinel-2 satellite images for monitoring cattle slurry and digestate spreading on emerging wheat crop: A field spectroscopy experiment. *Geocarto International* 38, 1 (2023), 2245371.
- [4] Andreas Kalogerias, Dimitrios Bompoudakis, Iason Tsardanidis, Dimitra A Loka, and Charalampos Kontoes. 2025. Monitoring digestate application on agricultural crops using Sentinel-2 Satellite imagery. *arXiv preprint arXiv:2504.19996* (2025).
- [5] Masahiro Kato, Fumiaki Kozai, and Ryo Inokuchi. 2025. PUATE: Semiparametric Efficient Average Treatment Effect Estimation from Treated (Positive) and Unlabeled Units. *arXiv preprint arXiv:2501.19345* (2025).
- [6] Sören R Küngel, Jasjeet S Sekhon, Peter J Bickel, and Bin Yu. 2019. Metalearners for estimating heterogeneous treatment effects using machine learning. *Proceedings of the national academy of sciences* 116, 10 (2019), 4156–4165.
- [7] Milan Kuzmanovic, Tobias Hatt, and Stefan Feuerriegel. 2023. Estimating conditional average treatment effects with missing treatment information. In *International Conference on Artificial Intelligence and Statistics*. PMLR, 746–766.
- [8] Tony Lancaster and Guido Imbens. 1996. Case-control studies with contaminated controls. *Journal of Econometrics* 71, 1-2 (1996), 145–160.
- [9] Bing Liu, Wee Sun Lee, Philip S Yu, and Xiaoli Li. 2002. Partially supervised classification of text documents. In *ICML*, Vol. 2. Sydney, NSW, 387–394.
- [10] Francesca Molinari. 2010. Missing treatments. *Journal of Business & Economic Statistics* 28, 1 (2010), 82–95.
- [11] Judea Pearl. 2009. *Causality*. Cambridge university press.
- [12] Judea Pearl and Dana Mackenzie. 2018. *The book of why: the new science of cause and effect*. Basic books.
- [13] Paul R Rosenbaum and Donald B Rubin. 1985. Constructing a control group using multivariate matched sampling methods that incorporate the propensity score. *The American Statistician* 39, 1 (1985), 33–38.
- [14] Donald B Rubin. 2005. Causal inference using potential outcomes: Design, modeling, decisions. *Journal of the American statistical Association* 100, 469 (2005), 322–331.
- [15] Jack D Saunders and Alex A Freitas. 2022. Evaluating the predictive performance of positive-unlabelled classifiers: a brief critical review and practical recommendations for improvement. *ACM SIGKDD Explorations Newsletter* 24, 2 (2022), 5–11.
- [16] Somya Sharma, Swati Sharma, Licheng Liu, Rishabh Tushir, Andy Neal, Robert Ness, John Crawford, Emre Kiciman, and Ranveer Chandra. 2023. Knowledge Guided Representation Learning and Causal Structure Learning in Soil Science. *arXiv preprint arXiv:2306.09302* (2023).
- [17] Dan Steinberg and N Scott Cardell. 1992. Estimating logistic regression models when the dependent variable has no variance. *Communications in Statistics-Theory and Methods* 21, 2 (1992), 423–450.
- [18] Elizabeth A Stuart. 2010. Matching methods for causal inference: A review and a look forward. *Statistical science: a review journal of the Institute of Mathematical Statistics* 25, 1 (2010), 1.
- [19] Ilias Tsoumas, Georgios Giannarakis, Vasileios Sitokonstantinou, Alkiviadis Koukos, Dimitra Loka, Nikolaos Bartsotas, Charalampos Kontoes, and Ioannis Athanasiadis. 2023. Evaluating digital agriculture recommendations with causal inference. In *Proceedings of the AAAI Conference on Artificial Intelligence*, Vol. 37. 14514–14522.
- [20] Ilias Tsoumas, Vasileios Sitokonstantinou, Georgios Giannarakis, Evangelia Lampliri, Christos Athanassiou, Gustau Camps-Valls, Charalampos Kontoes, and Ioannis N Athanasiadis. 2025. Leveraging causality and explainability in digital agriculture. *Environmental Data Science* 4 (2025), e23.
- [21] Hwanjo Yu. 2005. Single-class classification with mapping convergence. *Machine Learning* 61 (2005), 49–69.

813 A Real-World Datasets

814 For the sowing case, we follow the causal graph construction pre-
 815 sented in Tsoumas et al. [19], which guides the selection of relevant
 816 variables. In the fertilization case, we model the effect of fertilizer
 817 application on biomass production during the final phenological
 818 stages, incorporating both decisional and biological confounders.
 819 These confounders are selected based on a merged causal graph
 820 that combines the canonical fertilization–yield graph from Pearl’s
 821 book [12] with a more detailed soil-process causal graph from [16].
 822 Additionally, exogenous organic matter indexes, included as X vari-
 823 ables, are retrieved from the literature as features indicative of
 824 fertilization activity detectable by Sentinel-2 [3, 4]. As detailed in
 825 Table 3, adjustment variables (Z) cover the cultivation period up to
 826 01/05/2023, the treatment variable (T) indicates whether fertilizer
 827 was applied at least once between 01/09/2022 and 01/05/2023, and
 828 the outcome (Y) corresponds to NDVI-derived trapezoidal area be-
 829 tween 01/05/2023 and 30/06/2023, capturing the produced biomass
 830 at the end of the season.

832 B Simulation Datasets

833 We simulate data under two different structural assumptions. A
 834 **linear** setup and a **nonlinear** setup. In both cases, we generate
 835 $n = 1000$ samples.

837 Observed, Unobserved and Latent Variables

$$839 X_1, X_2, X_{11}, X_{22}, X_3, X_4, X_8 \sim \mathcal{N}(0, 1) \\ 840 U_1, U_2, U_3 \sim \mathcal{N}(0, 1) \\ 842 X_5 = 0.6U_1 + 0.6U_2 + \varepsilon_5, \quad \varepsilon_5 \sim \mathcal{N}(0, 0.1^2)$$

843 Linear Setup

845 Treatment Assignment.

$$846 \text{logit}(P(T = 1)) = 1.2X_1 + 0.8X_2 + 1.4X_{11} + 0.6X_{22} + 0.7X_4 + 1.0U_1 + 1.0U_3 \\ 848 T \sim \text{Bernoulli}(\sigma(\cdot)), \quad \sigma(z) = \frac{1}{1 + e^{-z}}$$

850 Mediator.

$$851 M = 1.5T + 0.7X_8 + 0.5X_2 + 0.3X_{22} + \varepsilon_M, \quad \varepsilon_M \sim \mathcal{N}(0, 0.1^2)$$

853 Outcome.

$$854 Y = 2.0M + 0.7X_1 + 0.5X_{11} + 0.6X_3 + 1.0U_2 + 1.0U_3 + \varepsilon_Y, \quad \varepsilon_Y \sim \mathcal{N}(0, 0.1^2)$$

856 Proxy Variables.

$$857 X_7 = 1.2M + \varepsilon_{X_7}, \quad \varepsilon_{X_7} \sim \mathcal{N}(0, 0.1^2) \\ 859 X_9 = 1.0T + 1.0Y + \varepsilon_{X_9}, \quad \varepsilon_{X_9} \sim \mathcal{N}(0, 0.1^2)$$

861 Nonlinear Setup

862 Treatment Assignment.

$$863 \text{logit}(P(T = 1)) = 1.2 \tanh(X_1) + 0.8 \sin(X_2) + 1.4 \tanh(X_{11}) + 0.6 \sin(X_{22}) \\ 865 + 0.7 \tanh(X_4) + 1.0U_1 + 0.8U_3X_1 \\ 866 T \sim \text{Bernoulli}(\sigma(\cdot))$$

868 Mediator.

$$869 M = 1.5T + 0.7\sqrt{|X_8|} + 0.5 \log(1 + |X_2|) + 0.3X_{22} + 0.1X_2X_8 + \varepsilon_M$$

871 Outcome.

$$872 Y = 2.0M^2 + 0.7X_1 + 0.5X_{11} + 0.6 \sin(X_3) + 0.2X_3^2 + 1.0U_2 + 1.0U_3 + \varepsilon_Y$$

873 Proxy Variables.

$$875 X_7 = 1.2M + \varepsilon_{X_7}$$

$$876 X_9 = 1.0T + 1.0Y + \varepsilon_{X_9}$$

877 In both setups, the variables X_7 and X_9 serve as proxies. X_7 for
 878 the mediator M , and X_9 as a collider involving both T and Y .

880 C Propensity scores

881 Following the figures for each experimental dataset with an overview
 882 of how propensity score overlap varies in the current experimental
 883 dataset when using different predictor sets (i.e X, Z) and methods
 884 (i.e. SPY, SPY + iSVM). This highlights how the choice of predictor
 885 variables and estimation approach affects the positivity assumption
 886 and common support.

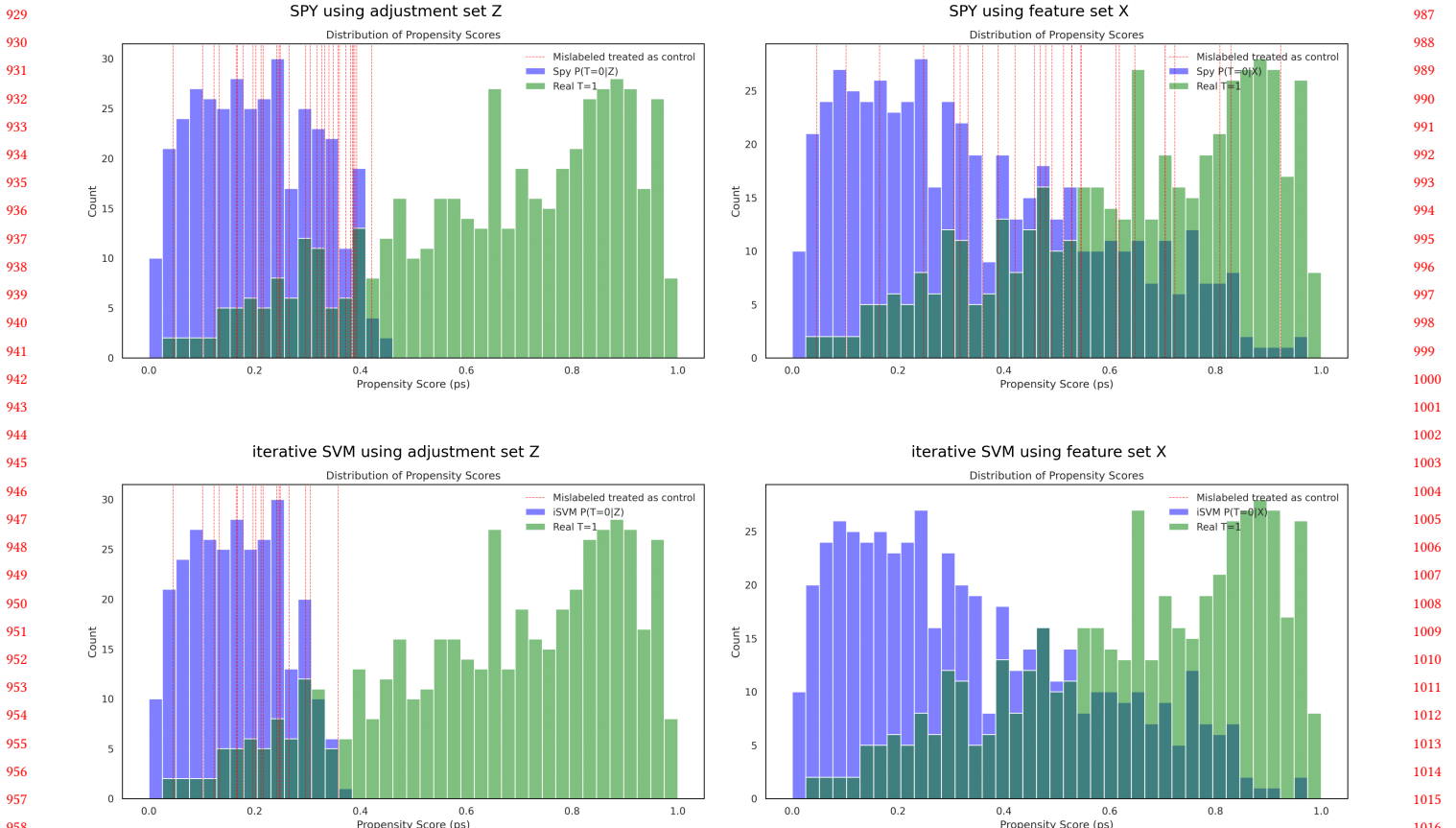


Figure 3: Propensity scores of 4 different combinations on linear experimental dataset

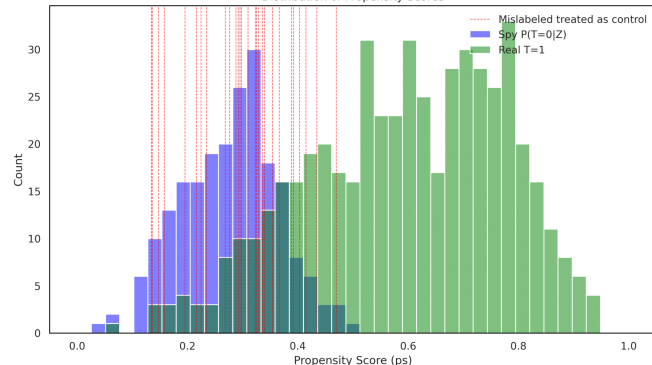
Sowing			Fertilization		
Feature(s) name	Variable/Vertex	Source	Set	Feature(s) name	Variable/Vertex
LOW, HIGH	Weather on sowing date	Nearest weather station	Z	SOC_prediction	Topsoil organic carbon (2022)
peak_ndvi_trapezoidal_ndvi_sow2harvest	Crop growth	NDVI via Sentinel-2	X	accum_precip_total_m	Accumulated precipitation (2022-09-01 - 2023-06-01)
ndwi_sowingday	Soil moisture on sowing date	NDWI via Sentinel-2	Z	gdd_base_0	Growing degree days (2022-09-01 - 2023-05-01)
clay_mean, silt_mean, sand_mean	Topsoil properties	Map by ESDAC	Z	ndmi_trapezoidal_area	Accumulated vegetation moisture content (2022-12-01 - 2023-05-01)
occont_mean	Topsoil organic carbon	Map by ESDAC	Z	sum_soil_moisture_mean	Soil moisture
var_{ST_402, ..., ELPIDA}	Seed variety	Farmers' Cooperative	Z	st_{Cambisols, ..., Luvisols}	ERA5-land
ratio	Geometry of field	Farmers' Cooperative	Z	POI_{[7807, ..., 10486]}	Soil type
lat, lon, perimeter, field_area	Location & area of field	Farmers' Cooperative	X	seed_{[1-4], nb2 - stats: max, min, mean, std, skew}	Seed variety
hdny_sin, hdny_cos, len_season	Harvest date & cultivation period	Farmers' Cooperative	X	Exogenous organic matter indexes	LPIs from NPA via Sentinel-2
prediction	Treatment (sown on recommended or not date)	Farmers' Cooperative, RS	T	TREATMENT	Fertilizer company
yield21	Outcome (Yield)	Farmers' Cooperative	X	ndvi_trapezoidal_area	NDVI via Sentinel-2

Table 3: Variables used for causal modeling in the sowing and fertilization case studies, categorized by their role (Z: adjustment set, X: features set, T: treatment, Y: outcome) and source.

1045

SPY using adjustment set Z

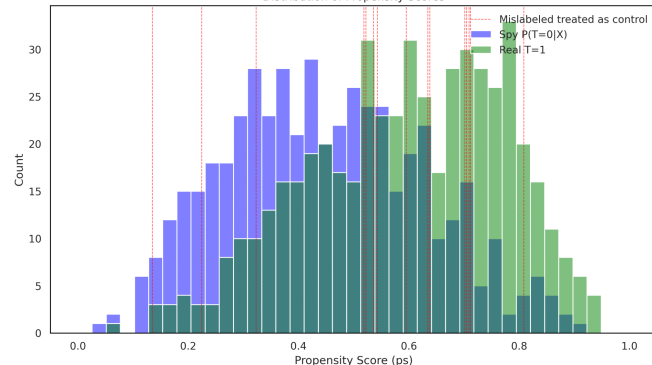
Distribution of Propensity Scores



1046

SPY using feature set X

Distribution of Propensity Scores



1047

1048

1049

1050

1051

1052

1053

1054

1055

1056

1057

1058

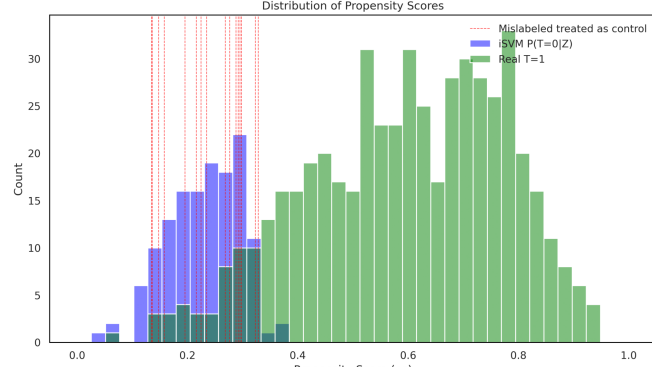
1059

1060

1061

iterative SVM using adjustment set Z

Distribution of Propensity Scores



1062

1063

1064

1065

1066

1067

1068

1069

1070

1071

1072

1073

1074

1075

1076

1077

1078

1079

1080

1081

1082

1083

1084

1085

1086

1087

1088

1089

1090

1091

1092

1093

1094

1095

1096

1097

1098

1099

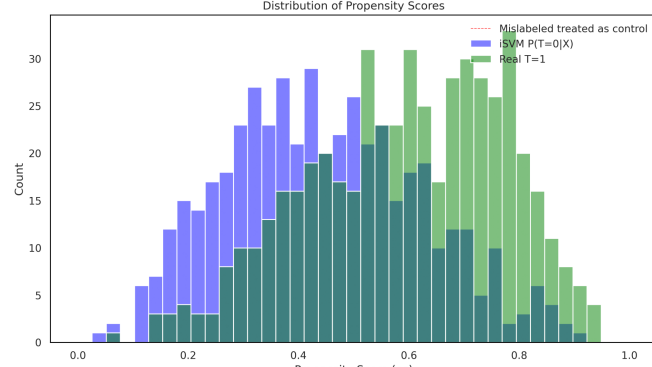
1100

1101

1102

iterative SVM using feature set X

Distribution of Propensity Scores



1103

1104

1105

1106

1107

1108

1109

1110

1111

1112

1113

1114

1115

1116

1117

1118

1119

1120

1121

1122

1123

1124

1125

1126

1127

1128

1129

1130

1131

1132

1133

1134

1135

1136

1137

1138

1139

1140

1141

1142

1143

1144

1145

1146

1147

1148

1149

1150

1151

1152

1153

1154

1155

1156

1157

1158

1159

1160

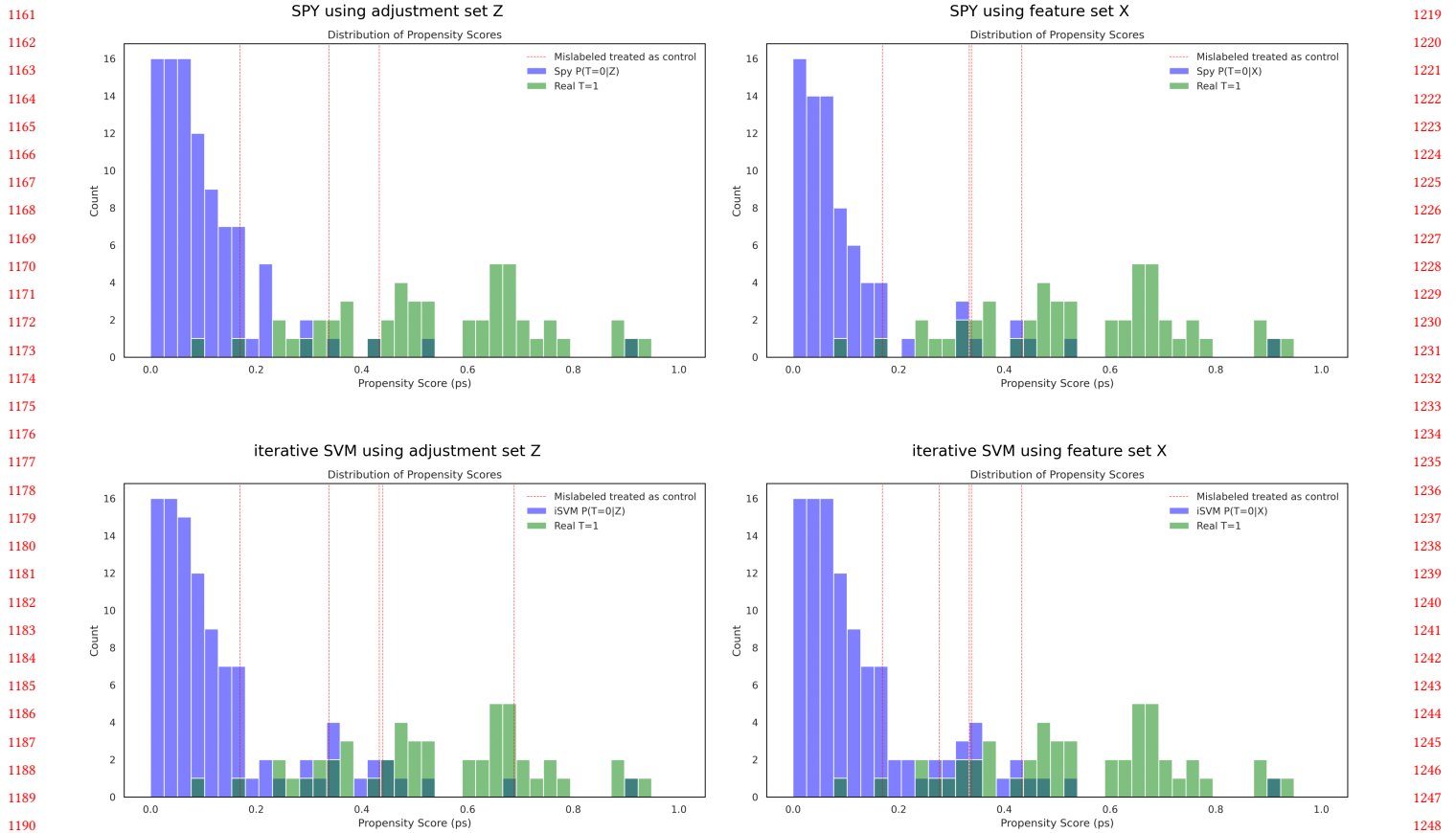
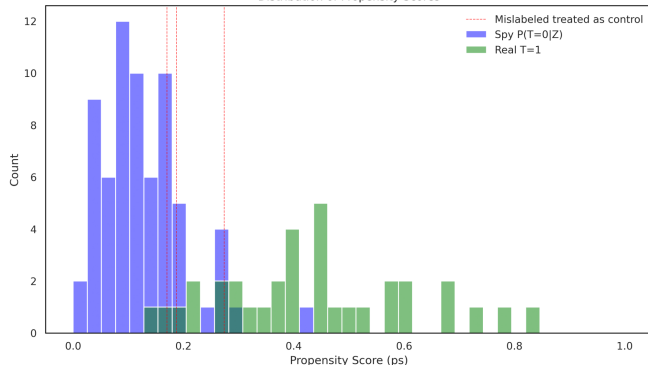


Figure 5: Propensity scores of 4 different combinations on experimental dataset regarding optimal sowing

1277

SPY using adjustment set Z

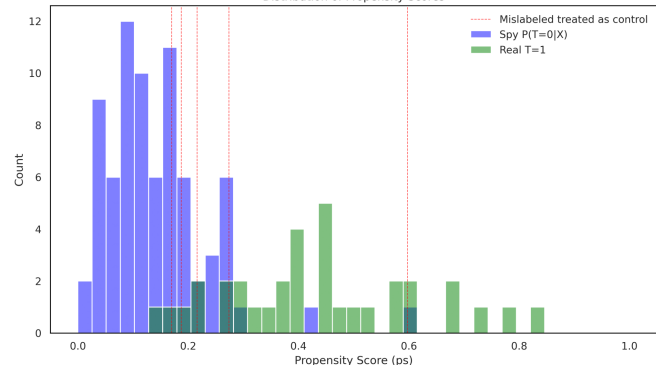
Distribution of Propensity Scores



1278

SPY using feature set X

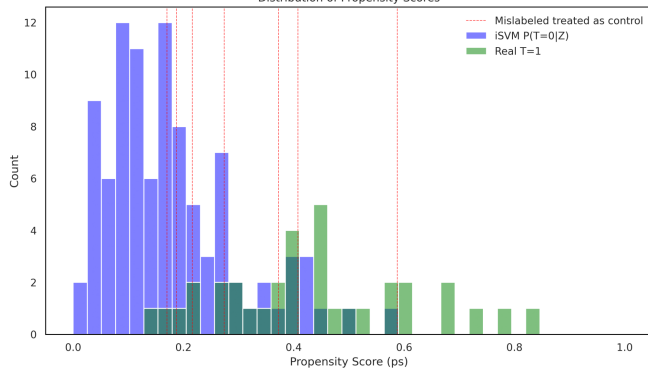
Distribution of Propensity Scores



1279

iterative SVM using adjustment set Z

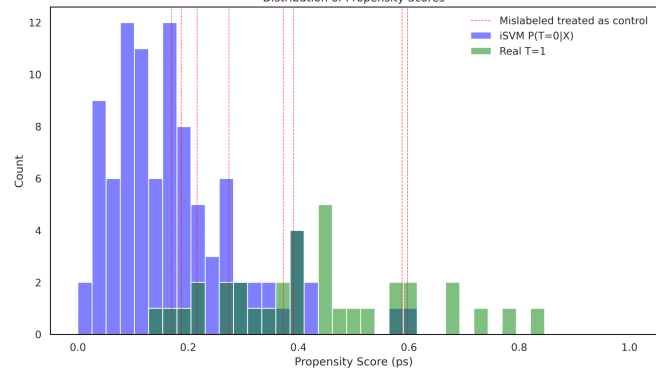
Distribution of Propensity Scores



1290

iterative SVM using feature set X

Distribution of Propensity Scores



1291

Figure 6: Propensity scores of 4 different combinations on experimental dataset regarding digestate fertilization application

1292

1293

1294

1295

1296

1297

1298

1299

1300

1301

1302

1303

1304

1305

1306

1307

1308

1309

1310

1311

1312

1313

1314

1315

1316

1317

1318

1319

1320

1321

1322

1323

1324

1325

1326

1327

1328

1329

1330

1331

1332

1333

1334

1335

1336

1337

1338

1339

1340

1341

1342

1343

1344

1345

1346

1347

1348

1349

1350

1351

1352

1353

1354

1355

1356

1357

1358

1359

1360

1361

1362

1363

1364

1365

1366

1367

1368

1369

1370

1371

1372

1373

1374

1375

1376

1377

1378

1379

1380

1381

1382

1383

1384

1385

1386

1387

1388

1389

1390

1391

1392

1393 D Interpretability and Model Comparison

1394 To investigate and compare the internal decision mechanisms of
 1395 two Support Vector Machine (SVM) classifiers, we examine the
 1396 learned feature coefficients from each model. Both classifiers share
 1397 a common architecture but differ in the feature sets used for training.
 1398 We leverage the linear nature of the SVM (with a linear kernel) to
 1399 extract and interpret feature importance directly from the model co-
 1400 efficients. These coefficients represent the influence of each feature
 1401 on the decision boundary—positive values contribute toward pre-
 1402 dicting the positive class (e.g., sowing on a good day), and negative
 1403 values contribute toward the negative class.

To visually communicate how feature importance shifts between
 the two models, we use a slope chart. Each line in the chart cor-
 responds to a feature, connecting its normalized coefficient in the
 model trained on adjustment set Z (left axis) to its corresponding
 value in the model trained of the superset of it, the feature set X
 (right axis). Features that are newly introduced in the superset X
 appear at zero on the left and are highlighted to emphasize their
 emergence in the decision function. Such comparative interpretability
 enhances our understanding of how additional information
 reshapes the model’s decision boundary..

Received 20 February 2007; revised 12 March 2009; accepted 5 June 2009

1404	1451
1405	1452
1406	1453
1407	1454
1408	1455
1409	1456
1410	1457
1411	1458
1412	1459
1413	1460
1414	1461
1415	1462
1416	1463
1417	1464
1418	1465
1419	1466
1420	1467
1421	1468
1422	1469
1423	1470
1424	1471
1425	1472
1426	1473
1427	1474
1428	1475
1429	1476
1430	1477
1431	1478
1432	1479
1433	1480
1434	1481
1435	1482
1436	1483
1437	1484
1438	1485
1439	1486
1440	1487
1441	1488
1442	1489
1443	1490
1444	1491
1445	1492
1446	1493
1447	1494
1448	1495
1449	1496
1450	1497
	1498
	1499
	1500
	1501
	1502
	1503
	1504
	1505
	1506
	1507
	1508

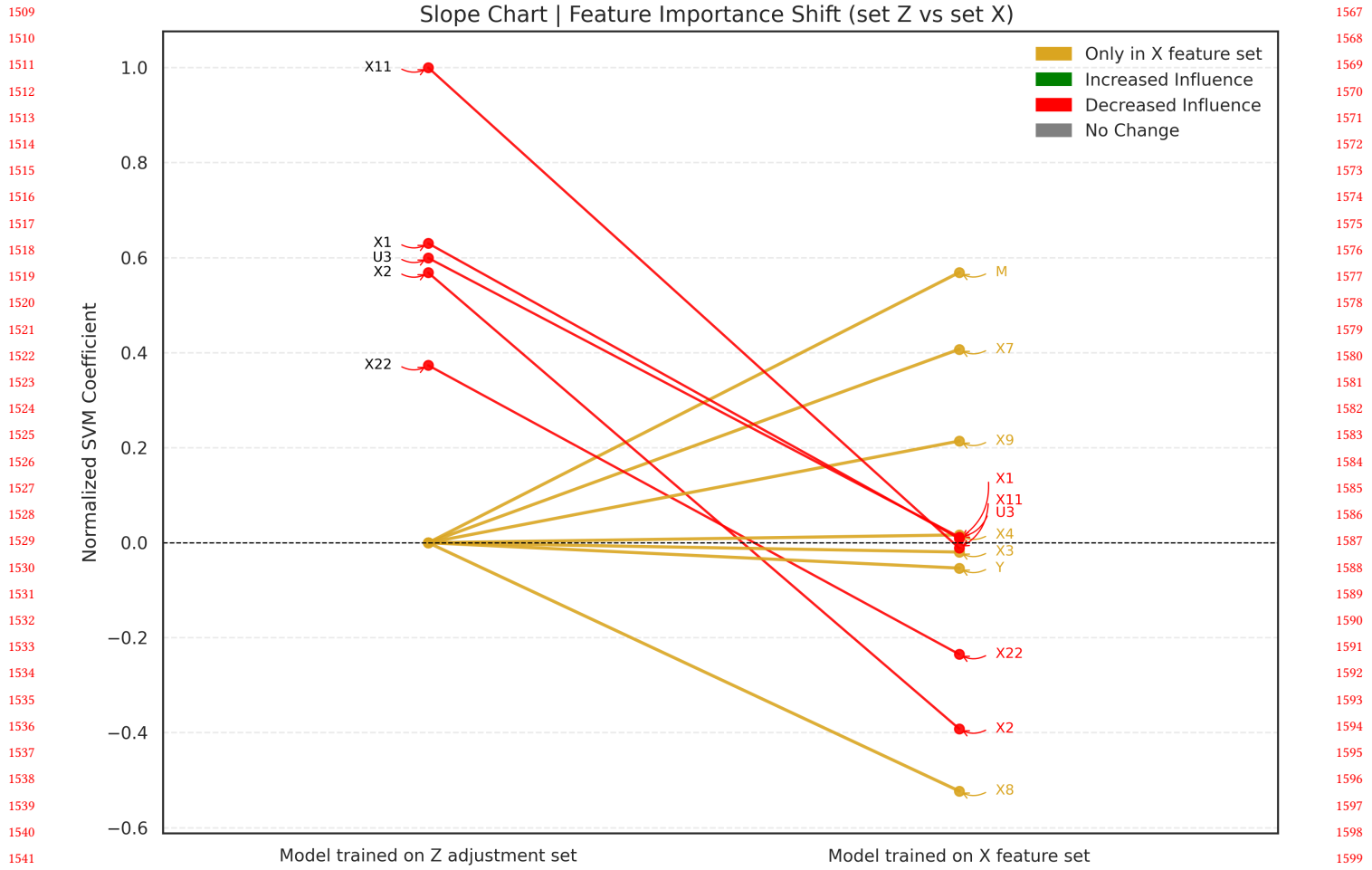


Figure 7: Interpretability and Model Comparison via SVM Coefficient Slope Chart for linear dataset

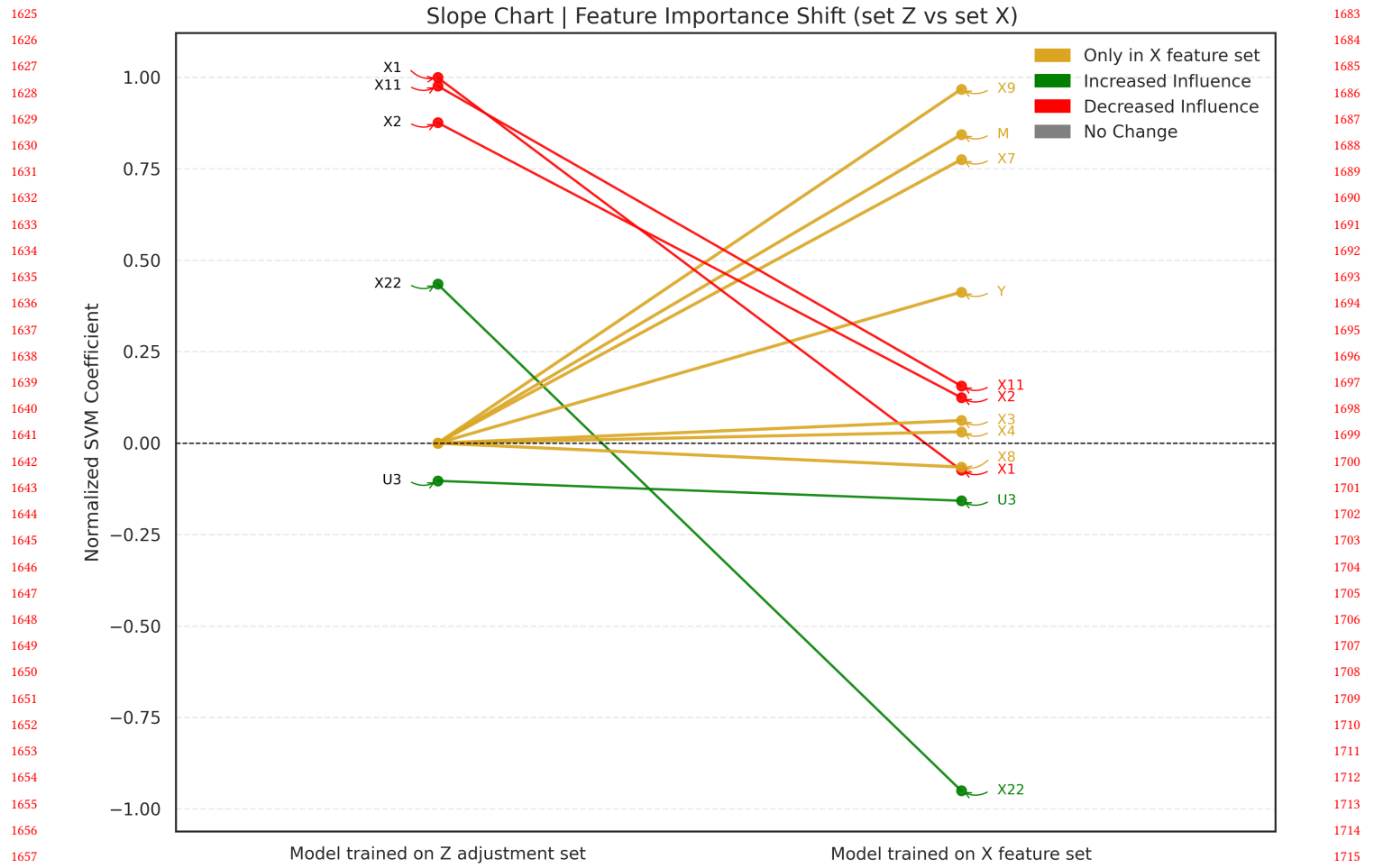


Figure 8: Interpretability and Model Comparison via SVM Coefficient Slope Chart for non-linear dataset

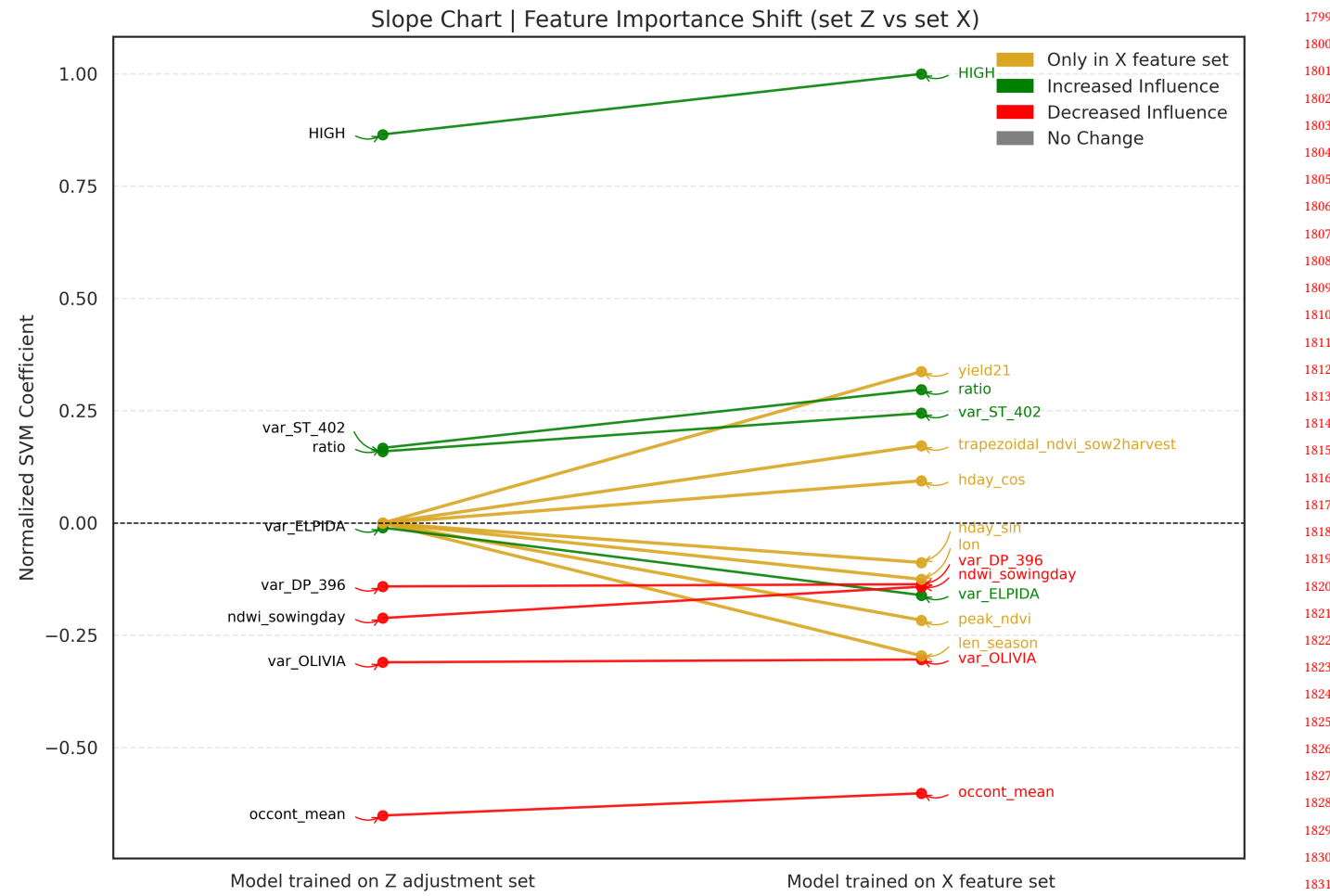


Figure 9: Interpretability and Model Comparison via SVM Coefficient Slope Chart for dataset regarding optimal sowing

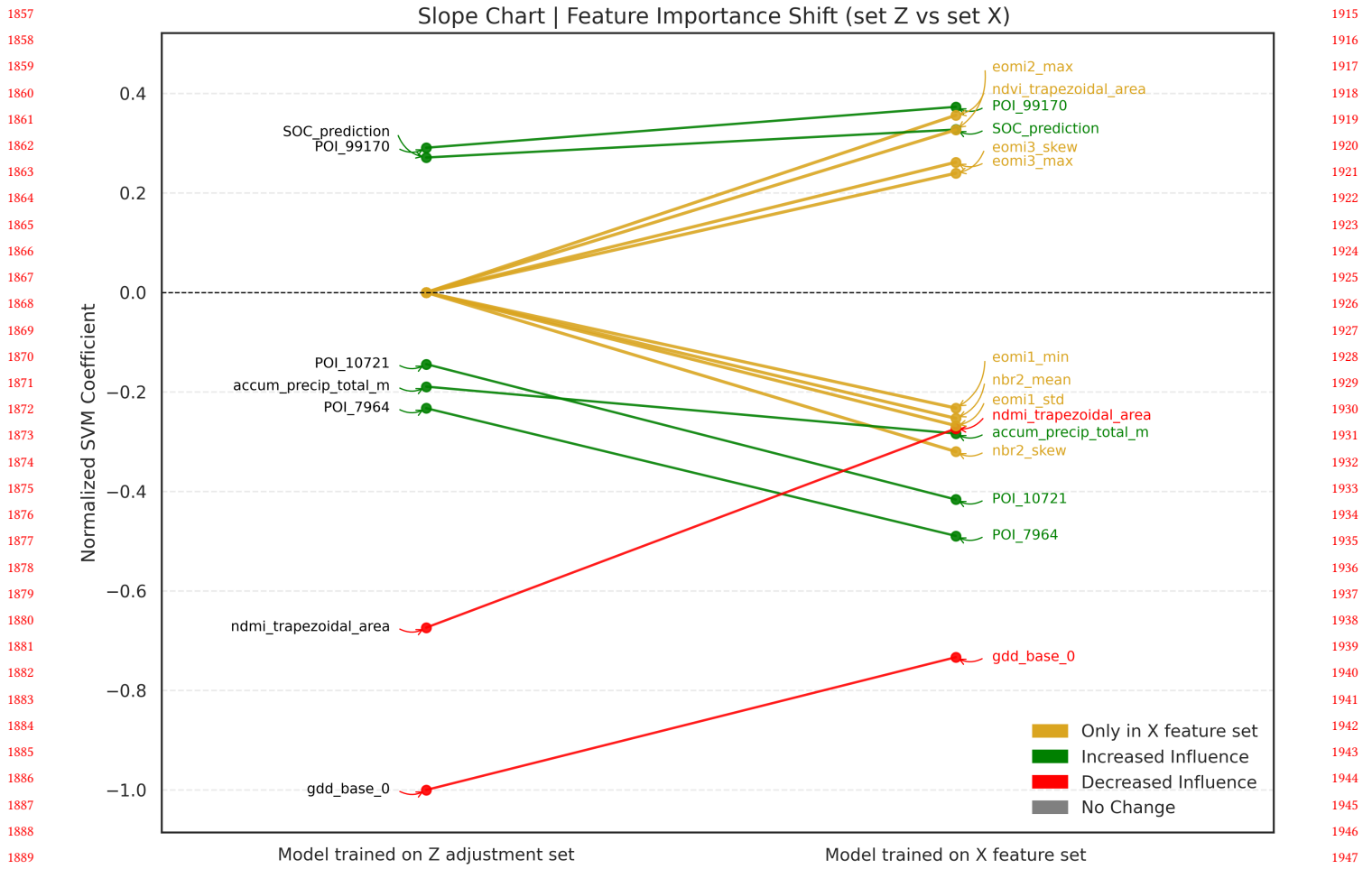


Figure 10: Interpretability and Model Comparison via SVM Coefficient Slope Chart for dataset regarding digestate fertilization application

1857
1858
1859
1860
1861
1862
1863
1864
1865
1866
1867
1868
1869
1870
1871
1872
1873
1874
1875
1876
1877
1878
1879
1880
1881
1882
1883
1884
1885
1886
1887
1888
1889
1890
1891
1892
1893
1894
1895
1896
1897
1898
1899
1900
1901
1902
1903
1904
1905
1906
1907
1908
1909
1910
1911
1912
1913
1914
1915
1916
1917
1918
1919
1920
1921
1922
1923
1924
1925
1926
1927
1928
1929
1930
1931
1932
1933
1934
1935
1936
1937
1938
1939
1940
1941
1942
1943
1944
1945
1946
1947
1948
1949
1950
1951
1952
1953
1954
1955
1956
1957
1958
1959
1960
1961
1962
1963
1964
1965
1966
1967
1968
1969
1970
1971
1972